Digest Journal of Nanomaterials and Biostructures Vol. 17, No. 3, July - September 2022, p. 825 - 837

Corrosion electrochemical behavior of arc sprayed Al coatings

Q. H. Song[a], Y. F. Zhang[a,*] Q. Li[b], Q.X.Li[b], C. Ju[a], Z. L. Wang[a], J. J. Li[a]
[a]*School of Mechanical Engineering, Qilu University of Technology (Shandong Academy of Sciences), Jinan, Shandong, 250353, PR China*
[b]*School of Material Science & Engineering, Qilu University of Technology, Shandong Academy of Sciences, Jinan, Shandong, 250353, PR China*

The Al coating was prepared on the surface of steel samples by arc spraying. The corrosion behavior of Al coating was analyzed by X-ray diffraction (XRD), scanning electron microscope (SEM), electromotive potential polarization and electrochemical impedance spectroscopy (EIS). The impedance data were fitted into an appropriate equivalent circuit to explain the electrochemical corrosion behavior of the coating in different stages. The micro morphology of arc sprayed Al coating surface was observed by SEM. It was found that the Al coating surface was in tentacle and layered structure, and the coating was porous and rough, which was related to the process of thermal spraying coating. XRD results showed that the oxide content in the coating was very small, and Al was the main component. The corrosion resistance of the coating was tested by EIS. The results showed that the Al coating had high corrosion resistance at the initial stage of corrosion, and a large number of bubbles were generated on the surface of the coating when it was immersed. Because there were many pores in the coating, which facilitated the penetration of Cl^-. However, with the extension of corrosion time, the coating first appeared pitting behavior. At this time, the outer surface of the corrosion hole formed an oxygen-rich area and became a cathode, and the concentration cell was formed outside the corrosion hole due to the decrease of oxygen concentration in the corrosion hole, which promoted the activation and dissolution of aluminum. The corrosion products of the coating will block the pores in the coatings, and the corrosion rate will decrease.

(Received April 18, 2022; Accepted July 22, 2022)

Keywords: Arc spraying, Al coating, Corrosion electrochemical behavior

1. Introduction

During using of steel bridges, they will be exposed to the atmospheric environment for a long time, and the steel bridges will be subject to atmospheric corrosion, seawater corrosion, soil corrosion and so on. Steel structure bridges not only bring convenience to people, but also bring cost problems to people. Corrosion is an inevitable phenomenon, which leads to fatigue effect and material damage of steel structure bridges, resulting in huge economic losses and casualties [1-3]. However, with the improvement of technical level, people can slow down the corrosion through

* Corresponding author: zhangyanfei@qlu.edu.cn
https://doi.org/10.15251/DJNB.2022.173.825

various methods. Thermal spraying has been continuously developed and innovated in recent years, and has become an important anti-corrosion measure, especially in the manufacture of anti-corrosion coatings on the surface of marine materials [4]. Arc spraying is a common method in thermal spraying technology, which is mainly used to prepare anticorrosive and wear resistant coatings for steel structures. This technique has good characteristics such as site constructability, low running costs, high spray rates and efficiency to coat large areas at the site [5-8]. Arc spraying is widely used in daily life, which can be used not only in indoor automatic spraying driven by servo motor, but also in outdoor manual hand-held spraying. Bridge construction period is long, the construction range is large, arc spraying is suitable for such construction conditions. In offshore oil wells, high temperature boilers, underground pipelines and other parts which are easy to be corroded but difficult to replace because of cost problems, spraying coating to improve the surface properties of the substrate has become a priority choice [9-10]. Aluminum is one of the most popular metal recommended for the protection of iron and steel from atmospheric corrosion and also for protection when immersed in salt and fresh water [11]. Aluminum coating as a protective coating for steel-based component products is generally considered to be a cheap and effective method, so it is widely used in various industries. Aluminum has good corrosion resistance and acts as sacrificial anode protection on the substrate. Passivation film will play a lasting role in protecting the substrate [12-15].

Thickness test, roughness test, wear resistance and corrosion resistance test were carried out on the composite coating composed of thermal spraying Al and anodic film. The wear resistance and corrosion resistance of the aluminum coating were significantly improved after anodic oxidation. The coating thickness increased with the increase of operation time, but the rough porous structure had no effect on the corrosion resistance, resulting in a significantly reduced AC impedance. The corrosion resistance of thermally sprayed aluminum was significantly improved after anodization, while the corrosion resistance of composite coatings decreased slightly with the increase of current density and operating time. Due to solidification, the use of anodized film effectively blocks the porosity of the coating, thereby slowing down the occurrence of corrosion. Erfan Abedi Esfahani [16] used the method of arc spraying to prepare Al coating on the surface of low carbon steel. The corrosion behavior of the coating in 3.5 wt.% NaCl solution was evaluated by EIS and polarization tests. Experiments showed that the corrosion current density of the Al coating was higher than that of the substrate. This may be due to the penetration of the electrolyte through the openings, resulting in accelerated aluminum corrosion. However, as the experiment progressed, corrosion products blocked part of the pores, resulting in a decrease in the corrosion rate. The test proved that the arc sprayed Al coating had good corrosion resistance [17].

2. Methods and procedure

2.1. Preparation of the coating

The substrate material was 304 steel sheet, the specification was 13 mm × 10 mm × 2 mm. 2.85 mm diameter of commercially pure 99.7 % Al wire was taken for coating. Before spraying, surfaces of the steel samples were grit blasted by white corundum under air pressure of 0.79 MPa to remove rust. After sand blasting, according to the national standard GB/T9793-1997

requirements, using QD8-D-400 spraying power supply equipment for spraying. The spraying process parameters were shown in Table 1, the final surface roughness was 7.13 um, and the coating thickness was 454 um. The entire spraying process took place indoors, preventing excessive oxidation as the coating forms. After spraying, the samples were air-cooled to room temperature to prevent large internal stress in the coatings. After the samples were collected, the samples were further analyzed.

Table 1. Arc spraying Al coating process parameters.

Coating meterial	99.7% Al
Air inlet pressure (MPa)	0.79
Spraying distance (mm)	150-160
Spraying voltage (V)	38
Spraying current (A)	220
Wire feed voltage (V)	22

2.2. Characterization

The Al coating sample was qualitatively analyzed on the D8 - ADVANCE (Germany) X-ray diffractometer (XRD) with continuous scanning at a scanning speed of 20° / min and a scanning range of 20 – 90°. The coating was inlaided with epoxy resin. After the resin was hardened, the samples were ground with 400 #, 600 # and 800 # SiC sandpaper, respectively.The samples were polished with HYP-1 universal metallographic sample polishing machine. The morphology and microstructure of the coating were characterized by ultra-high resolution scanning electron microscopy (GeminiSEM 500, Carl Zeiss, Germany).

Electrochemical tests were performed at room temperature using Interface1000 electrochemical workstation. The tests were carried out in the three-electrode mode. The working electrode was a sample with an exposed area of about 1cm^2. Reference electrode was saturated calomel electrode (SCE), the auxiliary electrode was a large area platinum sheet electrode.The corrosive medium was 3.5 wt.% NaCl solution, prepared with primary distilled water, and the reagents were of analytical grade. The scanning range was -0.25 - 1 V, the scanning speed was 0.166 mV / s, the frequency range was 0.01 Hz-100 kHz, and the initial stability time was 3600 s. After the open circuit potential was stable, the excitation signal was a sine wave with amplitude of 10 mV. The electrochemical impedance data were fitted and analyzed by Origin software.

3. Results and discussion

3.1. Coating characterization

The X-ray diffraction pattern of the coating was shown in Figure 1. The distinguishable phase is pure aluminum. Several crystal peaks appeared in the XRD pattern. According to the standard PDF card, these peaks corresponded to the α-Al crystal phase. No other phases except aluminum were detected in the XRD pattern, which may be due to the very low oxidation content, exceeding the detection limit of XRD.

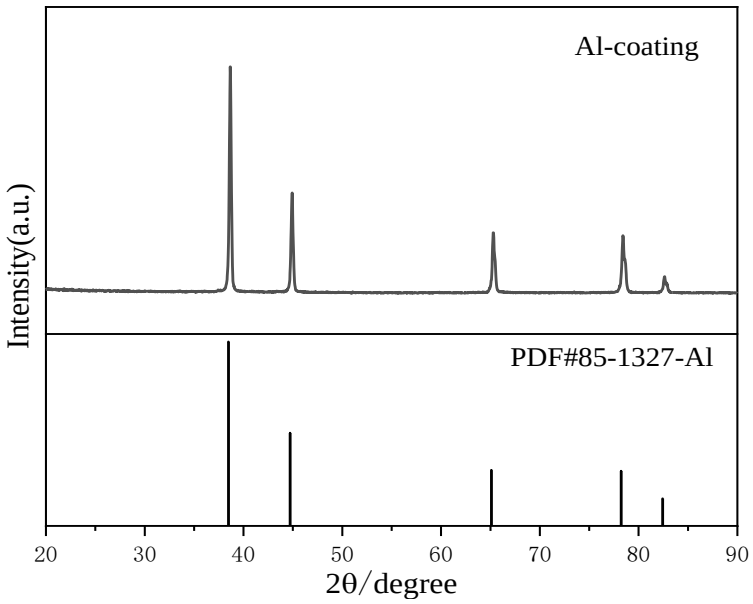

Fig. 1. XRD pattern of aluminum coating.

The microstructure of arc sprayed aluminum coating was shown in Figure 2. Figure 2a-c was the surface morphology of Al coating. It could be seen that there were many pores in the middle of the coating. The surface of the coating had obvious contact angle structure and the surface was rough and uneven. In the process of arc spraying, the aluminum wire was heated to a molten state by the arc, and the layers were superimposed on each other under the action of compressed air. Since the molten particles were sputtered to different degrees during the sputtering process, and certain pores were generated. It could be seen that there were many unmelted particles in the coating, and many deep pores appeared in the coating, which were in an open or semi-closed state. Figure 2e and Figure 2f were section and EDS of Al coatings, respectively. It could be seen that the cross-section of the coating and the substrate was serrated, which was a typical mechanical bonding form. Because in the process of grit blasting, irregular pits and surface points with certain roughness appeared on the matrix. The molten aluminum was sprayed to the substrate surface by atomization, filling the defects on the substrate surface. The thickness of the coating was about 450 um, and the coating was well bonded with the substrate without micro cracks. EDS showed that there were many tiny pores between the coatings, and the pores contain O. The coating contained a small amount of unmelted particles. The EDS elemental analysis of coating surface was shown in Figure 2d. Since the gas used in the spraying process was air, a small amount of oxidation will occur in the spraying process, which contained trace O. The main element on the coating surface was Al, and Al atoms appeared enrichment phenomenon. Some Fe and a small amount of Si were contained in the aluminum wire itself, and there was no oxidation behavior.

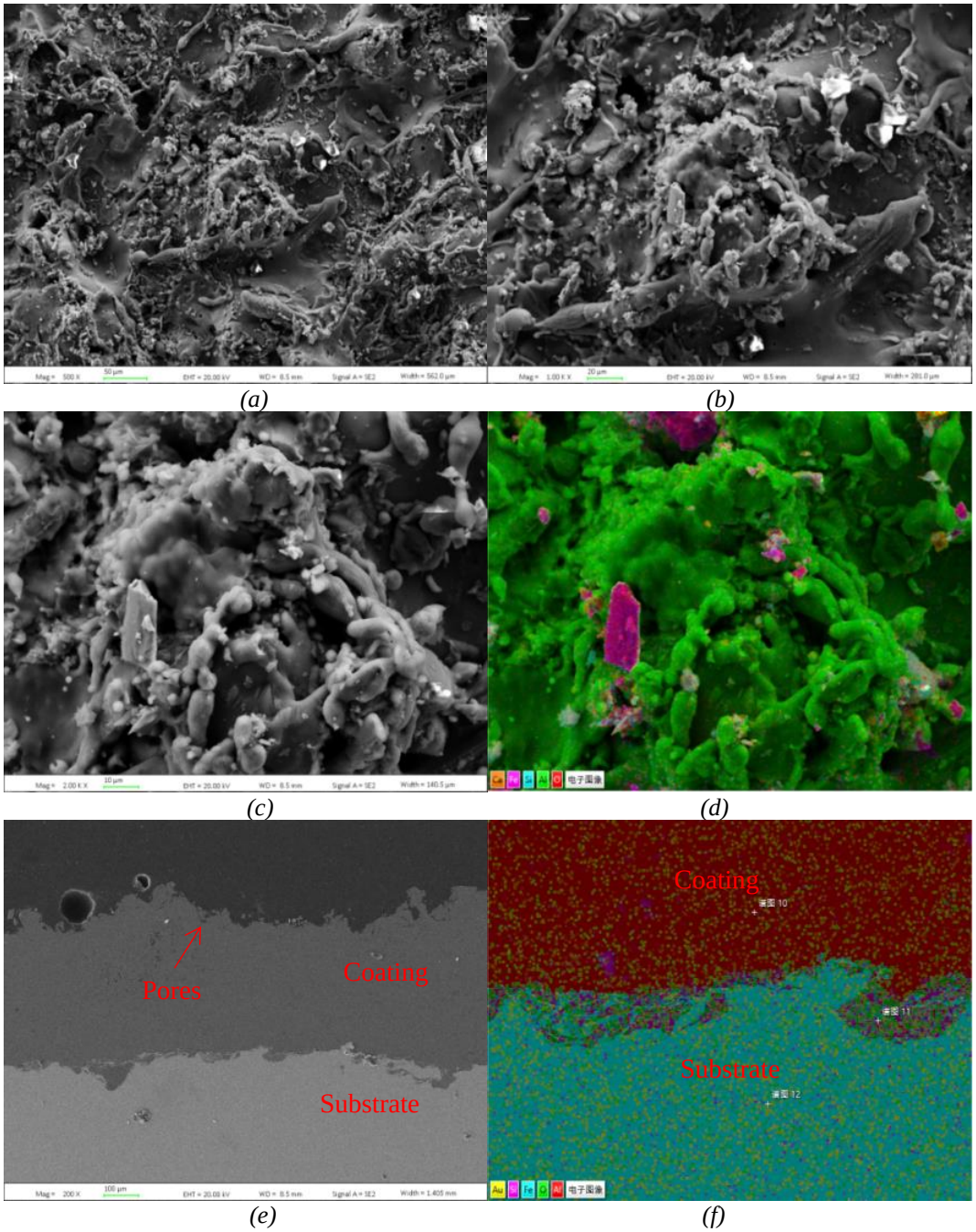

Fig. 2. Surface and cross scction of arc sprayed Al coating.

3.2. Corrosion performance of the coating

3.2.1 Tafel curve test

Figure 3 showed the potentiodynamic polarization curve of arc sprayed aluminum coating and substrate in 3.5 wt.% NaCl solution, which reflected the electrochemical behavior of the coating and substrate at the initial stage of corrosion. It could be seen that the self-corrosion potential of aluminum coating was significantly higher than that of steel substrate, and there was a tendency of passivation in the corrosion process. Tafel extrapolation method was used to extract the values of self-corrosion potential (E_{corr}) and corrosion current density (I_{corr}) from the curve. It

could be seen from Figure 3 that the self-corrosion potentials of aluminum coating and steel substrate were -0.1851 mV and -0.613 mV, respectively. Obviously, the self-corrosion potential of aluminum coating was higher than that of substrate. Corrosion potential was measured when the metal reached a stable corrosion state without external current. Corrosion potential reflected the thermodynamic trend of corrosion. It was a fixed value under a certain medium condition. The lower the corrosion potential value, the greater the possibility of material corrosion [18-19].

The corrosion current density reflects the dynamic characteristics of the corrosion process. Generally speaking, the higher the anodic polarization current density, the higher the corrosion rate. Therefore, the corrosion of the substrate is faster than that of the coating. Since the thermal spray coating inevitably forms pores during the preparation process, it can be seen in the Tafel curve that the coating first undergoes pitting behavior. The corrosion current density and corrosion rate of the coating and the substrate were measured by the Tafel extrapolation method. Table 2 showed the electrochemical corrosion performance parameters of the coating and the steel substrate in 3.5wt.% NaCl solution. It could be seen that the corrosion current densities of the steel substrate and the Al coating were 3.06×10^{-5} and 2.18×10^{-5} A·cm^{-2}, respectively, and the corrosion current density of the steel substrate was larger than that of the Al coating. The potentiodynamic polarization curve showed that the Al coating has an obvious protective effect on the substrate, which also verified the original intention of spraying the Al coating to prevent corrosion.

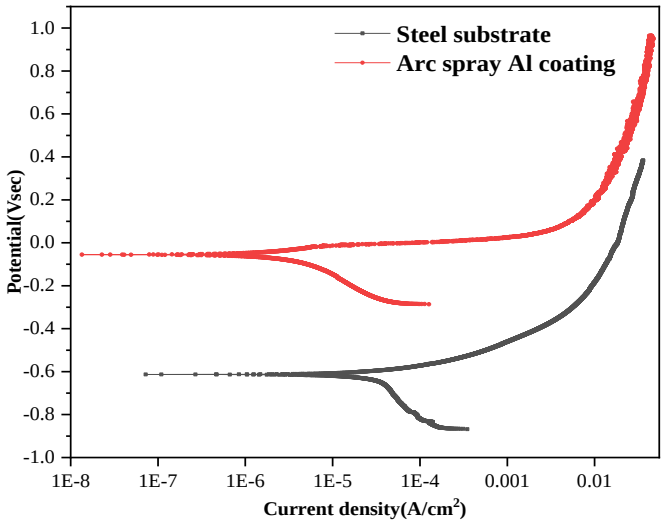

Fig. 3. Potentiodynamic polarization curves of Al coating and substrate in 3.5 wt.% NaCl solution.

Table 2. Corrosion properties of coatings in 3.5 wt.% NaCl solution.

Sample	E_{corr} (V)	I_{corr} (A/cm^2)
Steel substrate	-0.613	3.06×10^{-5}
Al coating	-0.1851	2.18×10^{-5}

3.2.2. EIS analysis of coating corrosion failure process

The corrosion resistance of arc sprayed aluminum coating is further studied by EIS. It is a

very useful technology, which can obtain the kinetics and mechanism of the corrosion process. According to the change of impedance diagram shape, the corrosion kinetics and mechanism of Al coating are described as follows.

Figure 4 and Figure 5 showed the Nyquist and Bode plots of Al coatings in 3.5 wt.% NaCl solution for different immersion times. Within 2 hours of immersion, the coating had a high protection rate. As a protective barrier, the corrosion medium did not reach the substrate interface. When the coating was formed, the molten metal will form pores in the splash process, and the corrosion solution will enter the pores of the coating with the increase of immersion time, so as to reach the substrate. The Nyquist diagram contained two arcs in the curves of 0 hour and 2 hours, and the Bode diagram contained two inflection points, indicating that there were two time parameters at this time, namely high frequency capacitive loop and low frequency capacitive loop. The high frequency capacitance loop corresponded to the corrosion product capacitance and corrosion product resistance, and the low frequency capacitance loop corresponded to the double layer capacitance and charge transfer resistance [20]. At this stage, the coating was initially dissolved and a thin layer of corrosion product film was formed on the surface, thus formed a double layer capacitance. The corrosion solution continuously entered the coating pores, deepening the original pores or forming new corrosion pits. The 2 days and 6 days impedance spectra showed a semicircle in the high frequency region, which was due to the simultaneous progress of the dissolution of the coating and the deposition of corrosion products on the surface of the coating, and the formation of a double-layer capacitance between the coating and the corrosion products. It indicated that the surface of the sample was smooth at this stage. The impedance value gradually decreased, and the phase angle moved to the low frequency direction, indicating that the film capacitance increased, and there was corrosion product deposition at the etching hole, blocking the entry of corrosion medium, so that the solution in the etching hole could not be diluted, thereby aggravating the corrosion of aluminum. The radius of Nyquist plot reached the maximum value at 6 days, indicating that the impedance value at this stage was the largest, and the corrosion product film had the strongest protective effect on the substrate. The fitting equivalent circuit of the corresponding electrode system was R(Q(R(QR))), as shown in Figure 6. Where R_s was the solution resistance, Q_f was the constant phase angle element at the uncoated surface / medium interface, R_f was the coating pore resistance, Q_d was the constant phase angle element at the interface reaction inside the pore, and R_t was the charge transfer resistance.

When the experiment was carried out from 12 days to 18 days, the corrosion solution continued to deepen along the pores of the coating, and the corrosion rate accelerated accordingly. As the corrosive medium diffused through the outer porous layer and penetrated into the interior of the coating, the phase angle decreased in the mid and low frequency range due to the formation of conductive percolation channels in the coating [21-22]. The corrosion products would be successfully diffused out, and the corrosion medium was exchanged in the pores. After 35 days of immersion, the solution became more and more turbid. Under the catalysis of corrosion medium, the Al coating continued to generate white flocculent substances, which were adsorbed on the surface of the coating and formed a certain protection for the coating. With increasing of immersion time, the corrosion holes in the deep part of the coating continued to expand, but the corrosion products generated by the sacrificial anode cannot be diffused, resulting in a large amount of accumulation, which played a sealing role in the coating. At this point, some holes had reached the substrate. The equivalent circuit of the electrode system at this stage was R(Q(R(Q(R(CR)))), as shown in Figure

7. Where R_{f1} was the surface pore resistance, Q_v was the constant phase angle element between the metal and the medium in the etching hole of the coating surface, R_{f2} was the pore resistance deep into the coating, C_a and R_t are the interface capacitance and reaction resistance between the metal and the medium that sacrificial anode dissolved in the etching hole deep into the substrate, respectively.

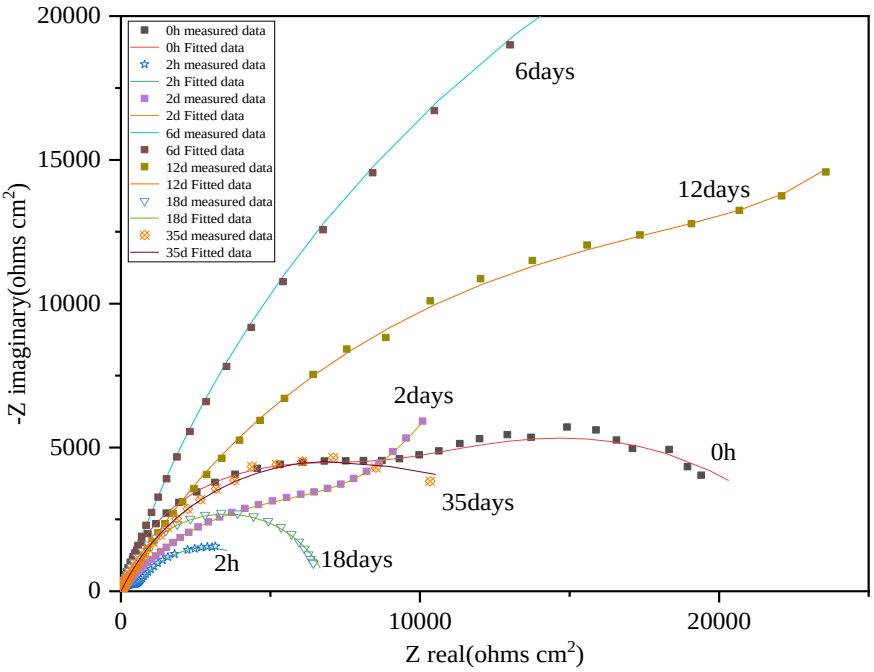

Fig. 4. Nyquist plot of Al coating in 3.5 wt.% NaCl solution for different immersion time.

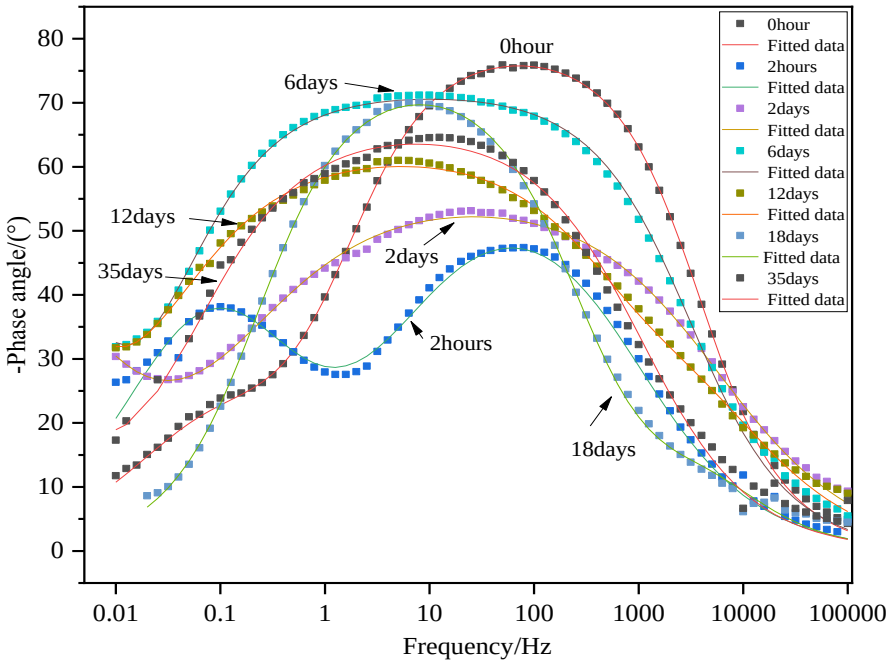

Fig. 5. Bode plots of Al coatings in 3.5 wt.% NaCl solution for different immersion times.

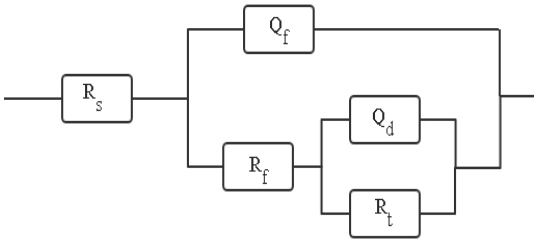

Fig. 6. EIS equivalent circuit model R(Q(R(QR))).

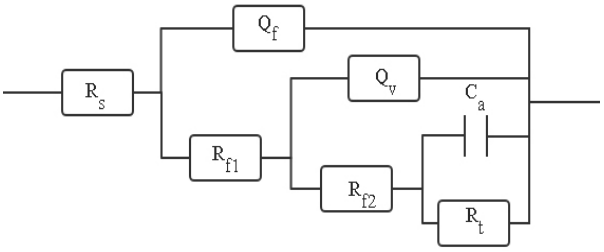

Fig. 7. EIS equivalent circuit model R(Q(R(Q(R(CR))))).

3.2.3. Morphology of the coating after corrosion

Figure 8 showed the surface morphology of aluminum coating after different soaking time. The corrosion of defects such as pores and cracks on the coating surface was mainly shown in Figure 8. It can be seen from Figure 8a-b that the coating had no obvious change, part of the tentacle-like structure had been dissolved, and the coating was smooth. At this time, the corrosion solution entered the pores of the coating, but did not reach the interface of the substrate, and the coating played a good role in the initial stage blocking effect. Because the Al coating formed an oxide film in the corrosive medium, which effectively slowed down the Cl^- penetration. There exhibited obvious pitting after immersing in 3.5 wt.% NaCl solution for 2 days (Figure 8c-d). Long spherical corrosion products appeared on the surface of the coating, but the coating remained intact without signs of falling off. A small amount of white substance appeared on the coating, as shown in region A. It can be seen from Figure 8e-f that the coating was honeycomb-like as a whole, and the white flocculent substances continued to accumulate on the surface of the coating, resulting in a large number of deposition, as shown in region B. Such deposition blocked the pores in the coatings, and corrosion and dissolution could not enter the coatings, showing short-term occlusion. The corrosion products mainly contained Al and O, forming aluminum oxides. The coating was honeycomb-like and the surface was rough after the 35 days immersion test, as seen from Figure 8g-i. It could be found that there were a small amount of crystals in addition to more white flocculent deposition. This was due to the dissolution of the coating during immersion, and the formation of Al_2O_3 and $Al(OH)_3$, which were adsorbed on the surface of the coating and hinder the corrosion medium from entering the pores of the coating. NaCl in the corrosion solution began to precipitate. Figure 8i was the surface EDS of the coating immersed for 35 days. It could be seen that the main elements on the surface were Na and Cl, and Al dissolved continuously in the process of immersion, resulting in a large number of Al oxides.

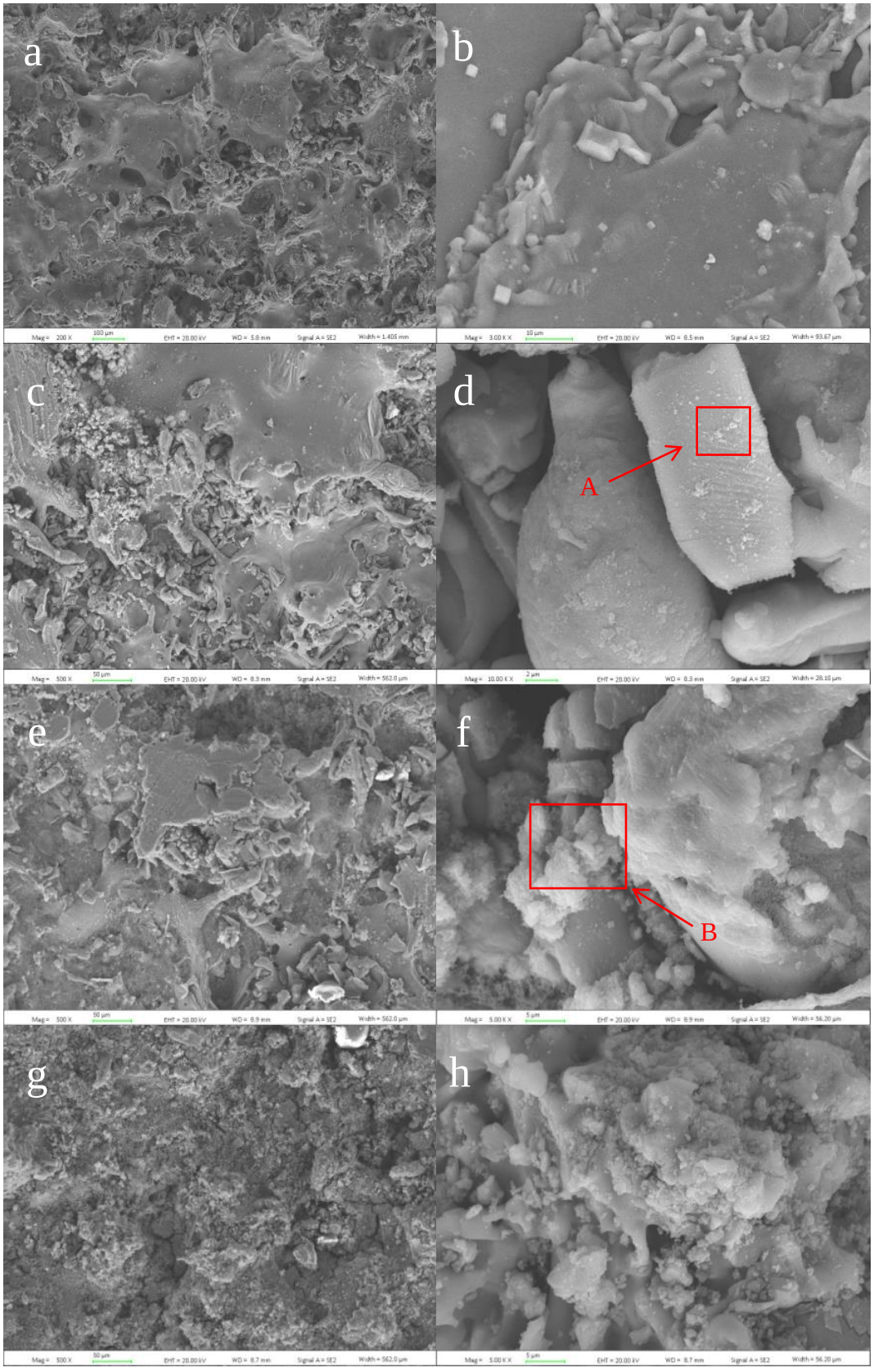
a
b
c
d
A
e
f
B
g
h

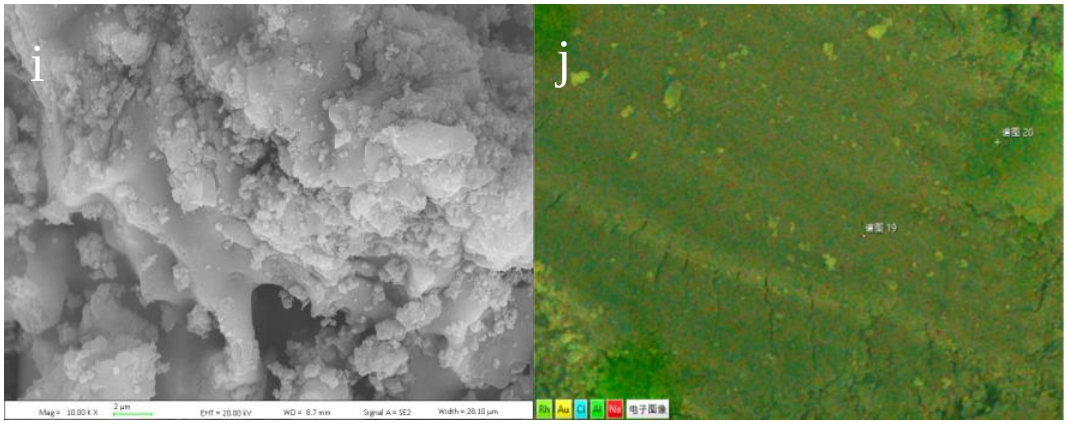

Fig. 8. Surface morphology of coatings after different immersion time: (a-b) immersion 2 hours; (c-d) immersion 2 days; (e-f) immersion 12 days; (g-i) immersion 35 days; (j) EDS of immersion 35 days.

Figure 9 showed the XRD pattern of the coating after 35 days immersion. The peak identification showed that the main phase in the coating was Al phase, and a small amount of NaCl adsorption. The corrosion solution was turbid and contains a large number of white flocculent substances. This material adsorbed on the surface of the coating, reducing the corrosion rate. Most of the generated oxides were precipitated in the solution, and only a small amount remained in the coating pores, which exceeded the XRD detection limit. It showed that during the immersion process of aluminum coating, oxides were constantly generated. The corrosion of medium on the coating was not achieved overnight, which was related to the thickness of Al coating.

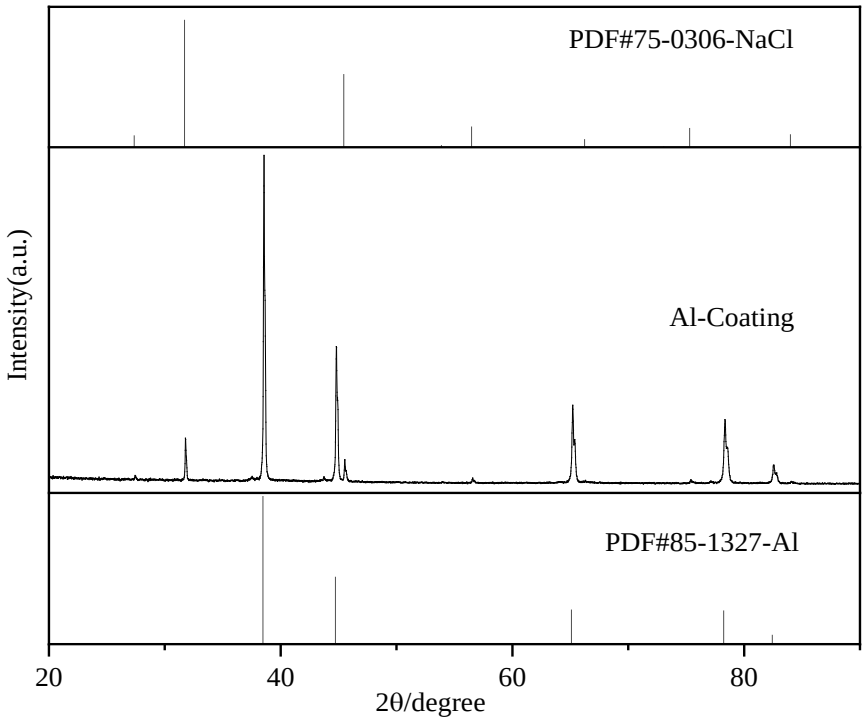

Fig. 9. XRD of the coating after 35 days immersion in 3.5 wt.% NaCl solution.

4. Conclusion

This study aimed to prepare anticorrosion coatings suitable for steel bridges by optimizing the process parameters of arc sprayed aluminum. The corrosion behavior of arc-sprayed Al coatings under simulated seawater conditions was investigated by electrochemical experiments. Compared with other thermal spraying methods, arc spraying was more suitable for large-scale construction.

The above experimental results showed that thermal spraying aluminum can effectively prevent the steel structure matrix from corrosion of simulated seawater solution. The SEM results showed that the microstructure of the sprayed aluminum coating was uniform, with typical layered structure and no obvious oxidation. The potentiodynamic polarization curves showed that the self-corrosion potential of the aluminum coating in 3.5 wt.% NaCl solution was smaller than that of the steel substrate, and the corrosion current density of the coating was larger than that of the substrate. The Al coating on the substrate surface could play a mechanical shielding protection role.The EIS test results showed that the coating had good anti-corrosion effect at the initial stage of corrosion. The electrolyte continuously entered the pores between the coatings, but the corrosion products blocked the pore defects, thus increasing the impedance value. However, with the extension of immersion time, the electrolyte reached the steel matrix through the pores of the coating, and corrosion damage occured. Experiments showed that the arc spraying aluminum coating can effectively protect the substrate from corrosion, and the substrate could also be effectively protected after 35 days of immersion. There were still large pores in the coatings, and there was a large space to improve the corrosion resistance of aluminum coatings. In further work and study, it is necessary to evaluate its corrosion resistance according to its actual needs.

Acknowledgements

The project was supported by “20 Policies about Colleges in Jinan” Program (Grant NO: 2019GXRC047), "migratory bird like" high level talent program in Tianqiao District and the provincial innovation and entrepreneurship training program of Qilu University of Technology (S202010431089).

References

[1] Rou. Li, Changqing. Miao, Yili. Zhang et al, Structures 34, 3414 (2021); https://doi.org/10.1016/j.istruc.2021.09.074

[2] Han. Xu, David Y. Yang, Dan. M..Frangopol, Engineering Structures 243, (2021); https://doi.org/10.1016/j.engstruct.2021.112633

[3] Yu. Zhang, Kaifeng. Zheng, Jin. Zhu et al, Construction and Building Materials 289, (2021); https://doi.org/10.1016/j.conbuildmat.2021.123108

[4] S.D. Zhang, J. Wu, W.B. Qi et al, Corrosion Science 110, 57 (2016); https://doi.org/10.1016/j.corsci.2016.04.021

[5] I1-Cho. Park, Seong-Jong Kim, Surface and Coatings Technology 325, 729 (2017);

https://doi.org/10.1016/j.surfcoat.2017.03.009

[6] C.H. Chang, M.C. Jeng, C.Y. Su et al, Thin Solid Films 517(17), 5265 (2009); https://doi.org/10.1016/j.tsf.2009.03.153

[7] Wengang. Chen, Zexiao. Wang, Guolin. Xu et al, Journal of Materials Research and Technology 15, 6562 (2021); https://doi.org/10.1016/j.jmrt.2021.11.084

[8] Muhamad. Hafiz. Abd. Malek, Nor. Hayati. Saad, Sunhaji. Kiyai. Abas et al, Procedia Engineering 68, 558 (2013); https://doi.org/10.1016/j.proeng.2013.12.221

[9] V.R.S. Sá Brito, I.N. Bastos, H.R.M. Costa, Materials and Design 41, 282 (2012); https://doi.org/10.1016/j.matdes.2012.05.008

[10] Xu. Wang, Dingyong. He, Xingye. Guo et al, Surface and Coatings Technology 367, 0257 (2019); https://doi.org/10.1016/j.surfcoat.2019.03.058

[11] H.Y. Li, J.Y. Duan, D.D. Wei, Surface and Coatings Technology 235, 259 (2013); https://doi.org/10.1016/j.surfcoat.2013.07.046

[12] Lijia Fang, Jing Huang, Yi Liu et al, Surface and Coatings Technology 357, 794 (2019); https://doi.org/10.1016/j.surfcoat.2018.10.094

[13] Heping. Li, Zhiqiang. Ke, Jing. Li et al, Journal of the European Ceramic Society 38(4), 1871 (2018); https://doi.org/10.1016/j.jeurceramsoc.2017.09.051

[14] Ze. Sun, Donghui. Zhang, Baoxu. Yan et al, Optics and Laser Technology 99, 282 (2018); https://doi.org/10.1016/j.optlastec.2017.09.013

[15] Qiong. Jiang, Qiang. Miao, Fei. Tong et al, Transactions of Nonferrous Metals Society of China 24(8), 2713 (2014); https://doi.org/10.1016/S1003-6326(14)63402-6

[16] Erfan. Abedi. Esfahani, Hamidreza. Salimijazi, Mohamad. A. Golozar et al, Journal of Thermal Spray Technology 21(6), 1195 (2012); https://doi.org/10.1007/s11666-012-9810-x

[17] Han-Seung. Lee, Jitendra. Kumar. Singh, Jang. Hyun. Park, Construction and Building Materials 113, 905 (2016); https://doi.org/10.1016/j.conbuildmat.2016.03.135

[18] Xiaoxia. Wang, Hang. Zhao, Songze. Wu, Journal of Materials Processing Technology 282, (2020); https://doi.org/10.1016/j.jmatprotec.2020.116642

[19] Y. Wang, S.L. Jiang, Y.G. Zheng et al, Surface and Coatings Technology 206(6), 1307 (2011); https://doi.org/10.1016/j.surfcoat.2011.08.045

[20] Chen. Haixiang, Kong. Dejun, Materials Chemistry and Physics 251, (2020); https://doi.org/10.1016/j.matchemphys.2020.123200

[21] Subrahmanya. Shreepathi, Priyansh. Bajaj, B.P. Mallik, Electrochimica Acta 55(18), 5129 (2010); https://doi.org/10.1016/j.electacta.2010.04.018

[22] Jia. Guo, Chengjia. Shang, Shanwu. Yang, Materials and Design 30(1), 129 (2009); https://doi.org/10.1016/j.matdes.2008.04.038